

Crystal Structure, Raman Spectroscopy, and Ab Initio Calculations of a New Bialkali Alanate K_2LiAlH_6

Ewa Rönnebro* and Eric H. Majzoub

Sandia National Laboratories, 7011 East Avenue, Livermore, California 94551-0969

Received: June 30, 2006; In Final Form: October 18, 2006

A new bialkali alanate K_2LiAlH_6 was synthesized at 320–330 °C and 100–700 bar. It was structurally characterized by powder X-ray diffraction. It crystallizes in space group $R\bar{3}m$ (No. 166) with unit cell parameters $a = 5.62068(8)$ and $c = 27.3986(6)$ Å. The Li and K cation sites are mutually exclusive, and Rietveld refinement finds no cation mixing. First-principles total energy calculations were performed for nine competing database structures of the stoichiometry A_2BCX_6 , taken from fluoride and oxide compounds in the Inorganic Crystal Structure Database (ICSD). The relaxed structures were compared via their total energies and their agreement with experimental diffraction spectra. Two database structures K_2LiAlF_6 ($R\bar{3}m$) and $\text{Cs}_2\text{NaAlF}_6$ ($C2/m$) were found to have the lowest total energies, but with the Rietveld method the K_2LiAlF_6 structure type was shown to be the most favorable. Ab initio total energy calculations support the validity of the structure determination. First-principles calculations also indicate that cation mixing is energetically unfavorable. Hydride properties such as plateau pressure are therefore more difficult to manipulate through alloying in this class of compounds.

1. Introduction

Many research groups are attempting to find new metal hydrides or other hydrogen storage materials that will meet the U.S. Department of Energy (DOE) system target of 6 wt % reversible hydrogen capacity at around 100 °C and 1–10 atm.¹ The classic intermetallic compound (IMC) metal hydrides, such as LaNi_5 , only reach about 1–2 wt %, while the complex metal hydrides, such as Mg_2NiH_4 and Mg_2FeH_6 , have higher hydrogen content (>3 wt %), but in general are not as easily reversible as the IMC hydrides. Therefore, the current research focus is on complex metal hydrides, which are reversible.

There are important differences between the IMC hydrides and the complex hydrides that are relevant to our results. The intermetallic compounds, such as AB_2 and AB_5 materials, are formed by combining strongly hydride forming transition metals (A) with more electronegative and non-hydride-forming metals (B). In IMC hydrides, hydrogen atoms enter interstitial tetrahedral or octahedral sites between the metal atoms. Alloying allows one to change both the size of the interstitial sites, and also their electron concentration, and thus modify the binding energy of the hydrogen interstitial.^{2,3} Because this binding energy is directly related to the equilibrium hydrogen overpressure, this results in the ability to tailor the plateau pressure of the compound to specific applications, at specific temperatures. The desired pressure is usually around 1 bar, at about 80 °C for proton exchange membrane (PEM) fuel cells.

In complex metal hydrides, hydrogen is bonded to a p- or d-element, forming an anionic complex, such as in AlH_6^{3-} or in FeH_6^{4-} , which is stabilized in a framework of cations of alkali or alkaline earth metals. Thus, complex metal hydrides contain metals with a higher electronegativity difference forming a stronger metal–hydrogen bond. The anionic complex is an isolated unit in a matrix of cations and is known in the literature to have several different geometries, such as octahedral,

tetrahedral, square-planar, or linear, and can take on various properties.⁴ Upon desorption of hydrogen, the metal atom structure is most often lost and cannot easily be reversed due to phase segregation and decomposition into binary hydrides, metals, or alloys. There are about 80 complex metal hydrides known in the literature.

Some of the most interesting complex hydrides are the alanates. For example, lithium alanate, LiAlH_4 , has a theoretical 7.97 wt % of hydrogen when decomposing to LiH , but has not been shown to be reversible. Potassium alanate, KAlH_4 , at 4.3 wt % when decomposing to KH , was shown to have reversible sorption properties in the range of 250–330 °C at pressures below 10 bar hydrogen without adding a catalyst.⁵ The most promising complex hydride to date is sodium alanate (NaAlH_4) containing 4.5 wt % reversible hydrogen at 100–200 °C when doped with a Ti-catalyst.⁶ NaAlH_4 is ultimately decomposed to NaH , with the hexahydride compound Na_3AlH_6 in the decomposition pathway. There are two Wyckoff sites for the Na-atom positions in the crystal structure of Na_3AlH_6 . This suggests that there may be stable bialkali alanates, or compounds with mixtures of alkali or alkaline earth elements forming the cation matrix around the AlH_6^{3-} anions. The structure and stability of some possible new alanates have been investigated using density functional calculations.⁷ Other groups have recently synthesized several bialkali alanates by solid-state reactions including $\text{Na}_2\text{-LiAlH}_6$, K_2LiAlH_6 , and K_2NaAlH_6 .^{8–10} The last compound crystallizes in the cubic elpasolite structure type in accordance with the theoretical predictions by Løvkvik and Swang.⁷

In section 3.1, we present the synthesis and crystal structure determination of phase pure K_2LiAlH_6 , with a crystal structure different from that obtained in ref 10. Confidence in the structure determination is enhanced through first-principles calculations, discussed in section 3.3, of the Rietveld-refined structure, and competing structures taken from a crystal structure database, which show the Rietveld-refined structure to have the lowest total energy. We find that the two cations involved in the stabilizing matrix are located in mutually exclusive Wyckoff

* Corresponding author. E-mail: ecronne@sandia.gov.

TABLE 1: Atomic Parameters for K_2LiAlH_6 in Space Group $R\bar{3}m$ (No. 166)^a

atom	Wyckoff position	x	y	z	B (Å ²)
Li	6c	0	0	0.4036(8)	1.9(5)
Al1	3a	0	0	0	3.35(8)
Al2	3b	0	0	1/2	3.22(9)
K1	6c	0	0	0.1270(1)	2.57(6)
K2	6c	0	0	0.2853(1)	2.25(6)
H1	18h	0.096(7)	−x	0.466(3)	0.75
H2	18h	0.205(5)	−x	0.638(2)	4.7

^a $a = 5.62068(8)$ and $c = 27.3986(6)$ Å from Rietveld refinements. Standard deviations are shown in parentheses.

positions and not mixed on the same site. This has also been found to be true for other quaternary systems and indicates any thermodynamic tuning through cation mixing is unlikely in $\text{K}_2\text{-LiAlH}_6$.^{4,11} In section 3.2, we provide Raman spectra of phase pure K_2LiAlH_6 , and also with a mixture of KAlH_4 for comparison. The Al–H vibrations in the spectra indicate the difference in Al–H coordination number and bond strength.

2. Experimental Section

2.1. Synthesis Method. A 2 g mixture of LiAlH_4 :KH in the ratio 1:2 was prepared by ball milling under argon in a SPEX8000 high-energy mill using six 9 g WC milling balls for approximately 30 min, or alternatively hand ground with a mortar and pestle. All sample handling was performed in an argon-filled glove box equipped with oxygen and moisture sensors to monitor the O_2 and H_2O content, which was less than 1 ppm. The powders were then pressed into pellets of 10 mm diameter in a hydraulic Carver press and placed in two-part sample crucibles made of stainless steel (dimensions: $H = 30.15$ mm and $D = 28.58$ mm). The top part is equipped with a 10 μm filtered opening to allow the hydrogen gas to diffuse into the sample. The crucibles were placed in an AE Closure (Snap-tite, Inc.), a self-sealing vessel of nominal capacity of 100 mL that utilizes internal pressure to tighten the seal. The new phase appeared after heat treating the mixture at 320–330 °C and 700

bar for 1–2 days. The sample was then cooled under pressure and removed under argon. The pellet changed color from gray to white, and the pellet diameter expanded.

Using this technique, we attempted to synthesize compounds in the following systems, Li–Mg–Al–H, Li–Ca–Al–H, Li–Ti–Al–H, and Mg–Ti–Al–H, with up to 1500 bar H_2 -pressure. These attempts were unsuccessful.

2.2. Powder X-ray Diffraction Analysis and Rietveld Refinements. For phase identification, X-ray powder diffraction data were collected on a rotating anode Rigaku diffractometer (RU-300) with a Cu-target at 40 kV and 40 mA at 295 K. The powder was contained in a 0.7 mm diameter vacuum-grease sealed capillary. After a peak list without impurities (small amount of KH, no oxides) was prepared, the trial-and-error program TREOR was utilized to find the unit cell dimensions.¹² The Rietveld method was used to verify the atomic positions using the program Fullprof.¹³ Refined parameters were zero-point, scale factor, unit cell parameters, UVW, atom positions, and displacement factors. The background was modeled by interpolation between manually chosen points.

2.3. Raman Spectroscopy. Raman data were collected on a Spex model 1877 0.6 m triple spectrometer, using the 514 nm line of a Coherent Innova Ar ion laser, at a power of about 10 mW at the sample. All spectra were collected in 180° back-scattering geometry utilizing a microprobe apparatus consisting of a 20× objective to focus the incident light and collect the scattered light. Samples were housed in an argon-filled quartz cuvette.

2.4. Ab Initio Calculations. Total energy calculations were performed using the Vienna Ab initio Simulation Package (VASP).¹⁴ Perdew–Burke–Ernzerhof (PBE) generalized gradient (GGA) pseudopotentials¹⁵ were used with a plane wave energy cutoff of 400 eV. The Brillouin zone for each structure was sampled with a Monkhorst–Pack mesh using a k -point spacing of less than 0.05 Å^{−1}. Structures for total-energy comparisons were taken from the Inorganic Crystal Structure Database (ICSD),¹⁶ which had stoichiometry analogous to that of the prepared material K_2LiAlH_6 . The ICSD structures were relaxed via VASP until the atomic forces were less than 0.01

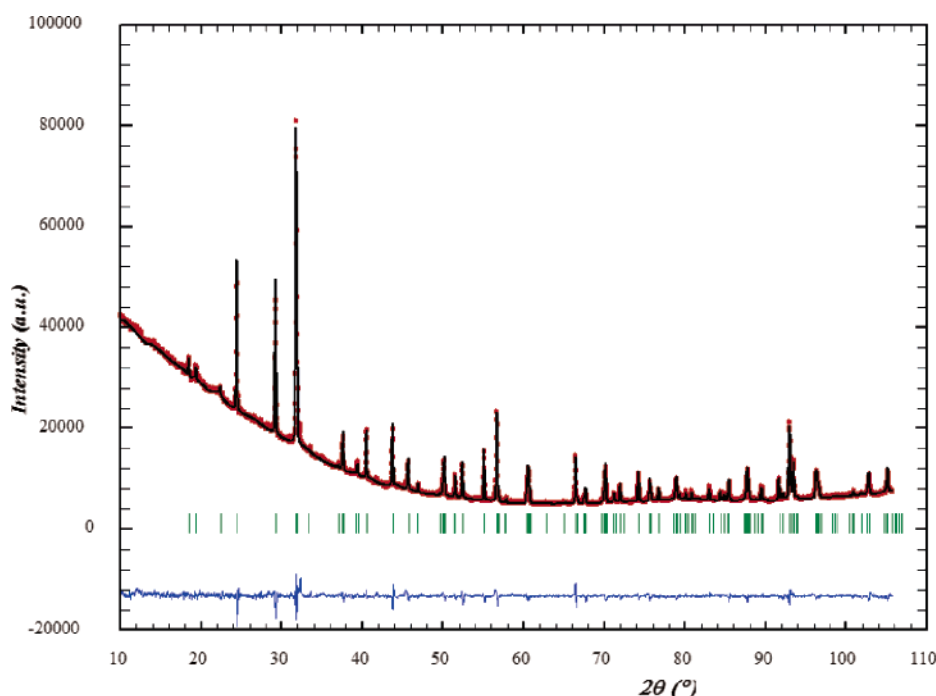


Figure 1. The observed and calculated X-ray patterns with the difference plot from Rietveld refinements of K_2LiAlH_6 .

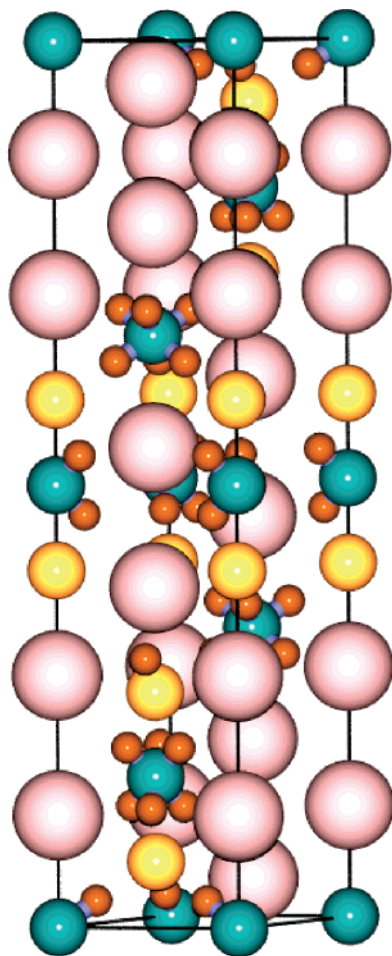


Figure 2. The crystal structure of K_2LiAlH_6 . Potassium is shown in pink, lithium in yellow, and aluminum in green. Atom Al1 is in Wyckoff position (0,0,0), while Al2 is in position (0,0, $1/2$). The four Al atoms located halfway up the c -axis, and one each closest to the plane $z = 0$ and $z = 1$, are in the Al2 position.

$\text{eV}/\text{\AA}$. Changes in the cell volume during relaxation will change the effective cutoff energy; therefore, the calculations were repeatedly restarted until no further cell minimization took place. The output structures were analyzed for new or changed symmetries using the SYMSEARCH program from the ISOTROPY software package.¹⁷

3. Results and Discussion

3.1. Crystal Structure. From the literature, the structure of K_2LiAlH_6 synthesized by mechanical alloying was reported by Graetz et al.¹⁰ to be isostructural with the low-temperature form of K_2LiAlF_6 , cubic elpasolite ($Fm\bar{3}m$), but the XRD data were not of sufficient quality to allow Rietveld refinement, and thus a final conclusion on the structure was not possible. Løvvik and Swang predicted the structure of K_2LiAlH_6 to be of face-centered cubic symmetry in accordance with the low-temperature phase of K_2LiAlF_6 .⁷

From our X-ray diffraction data, a small monoclinic unit cell of space group $P2_1/m$ (No. 11) was suggested by the program TREOR.¹² The unit cell was refined to $a = 9.279(5)$ \AA , $b = 2.8114(7)$ \AA , $c = 4.876(4)$ \AA , and $\beta = 100.06(5)^\circ$ with a figure of merit of $M_{20} = 24$ using the program Pirum.¹⁸ An attempt was made to refine different reasonable atomic positions from International Tables of Crystallography¹⁹ for K and Al with the Rietveld refinement program Fullprof,¹³ but without obtaining a satisfying fit between observed and calculated pattern.

TABLE 2: Shortest Metal–Hydrogen-Bonding Distances [\AA] in K_2LiAlH_6 from the Rietveld Refinements of Type Structure HT- K_2LiAlF_6

bond	distances [\AA]			
Li–H	1.94844	2.29828		
Al–H	1.31956	1.47574		
K1–H	2.89748	2.96978		
K2–H	2.88424	2.89813	3.06794	3.27345
H1–H1	1.61876	2.08437	2.63913	
H2–H2	2.00711	2.16396	2.95148	

Therefore, the program SHELXS97 was used in an attempt to find the heaviest atom positions with the Patterson method,²⁰ but the obtained coordinates still could not be refined in Fullprof.

However, there is a high-temperature form of K_2LiAlF_6 , which crystallizes in the hexagonal-rhombohedral $\text{Cs}_2\text{NaCrF}_6$ -type structure, with space group $R\bar{3}m$ (No. 166) (Table 1). By comparing the XRD pattern of our synthesized compound with the spectra in the paper by Arndt et al.,²¹ it was concluded that the structure of our new alanate is likely isostructural with the hexagonal-rhombohedral K_2LiAlF_6 . Because of its large unit cell, it was not suggested as a solution by TREOR, even though it has higher symmetry. Using the high-temperature fluorite structure, the X-ray pattern was refined with the Fullprof program.¹³ The cell parameters were refined in space group $R\bar{3}m$ ($Z = 6$) to $a = 5.62068(8)$ and $c = 27.3986(6)$ \AA . R -values of $R_B = 9.57\%$ and $R_F = 8.36\%$ were obtained for the metal atom structure. When adding the two H-sites, the R -values decreased to $R_B = 8.41\%$, $R_F = 7.41\%$, and $R_{WP} = 3.72\%$. The observed, calculated, and difference plots from the Rietveld refinement are shown in Figure 1. The structure of K_2LiAlH_6 is shown in Figure 2.

In the following, we will compare the Rietveld-refined metal–H bond distances in K_2LiAlH_6 with the D–metal bond distances in alanates, which are available in the literature (Table 2). The Li–H distances in K_2LiAlH_6 , from the refinement, are 1.94–2.24 \AA , in comparison to 1.89–2.12 \AA for Li–D in Li_3AlD_6 ,²² and 1.83–1.94 \AA for Li–D in LiAlD_4 .²³ The Al–H distances in K_2LiAlH_6 , from the refinement, are 1.31–1.47 \AA , which is somewhat shorter than in the other alanates. The Al–D distance is 1.73 \AA in Li_3AlD_6 ,²² 1.60 \AA in LiAlD_4 ,²³ 1.63 \AA in NaAlD_4 ,²⁴ 1.75 \AA in Na_3AlD_6 ,²⁵ and 1.62 \AA in KAID_4 .²⁶ The K–H distances in K_2LiAlH_6 , from the refinement, are 2.89–3.07 \AA as compared to 2.60–3.18 \AA for K–D in KAID_4 .²⁶ There are two slightly distorted octahedra of hydrogen surrounding two crystallographically distinct sites of Al in the structure. The AlH_6 octahedra appear to be more distorted than the corresponding octahedra in K_2LiAlF_6 , as was also found to be true for NaMgH_3 and NaMgF_3 .²⁵ For comparison with the hydride, the bonding distances in HT- K_2LiAlF_6 are 1.96–2.16 \AA for Li–F, 1.80–1.81 \AA for Al–F, and 2.74–3.05 \AA for K–F.²⁷ The Al1 atom surrounded by six hydrogen (H2) atoms has the following bonding distances: Al–H2 1.48 \AA , H2–H2 2.01, 2.16, and 2.95 \AA , and H2–Al–H2 angles 85.7°, 94.3°, and 180.0°. The Al2 atom surrounded by six H1 atoms is more distorted: bonding distances Al2–H1 1.32 \AA , H1–H1 1.62, 2.09, and 2.64 \AA , and H1–Al–H1 angles 75.7°, 104.3°, and 180.0°. Because of the low scattering factor for hydrogen, it is likely that the refined atomic coordinates are only approximate, leading to two different representations of the aluminum octahedral.

3.2. Raman Spectroscopy. The difference in Al–H coordination number between the AlH_4^- and AlH_6^{3-} anions in the compounds K_2LiAlH_6 and KAH_4 should be apparent through the difference of the Al–H stretching frequencies. Therefore,

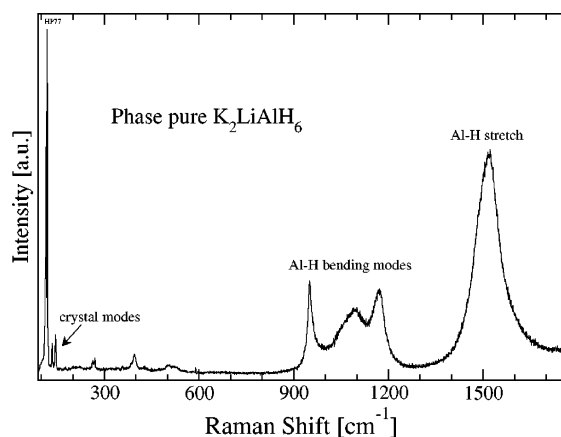


Figure 3. Raman spectrum of pure K_2LiAlH_6 . The Al–H bending modes lie between 900 and 1200 cm^{-1} . The stretching modes of the AlH_6^{3-} anion are centered near 1500 cm^{-1} .

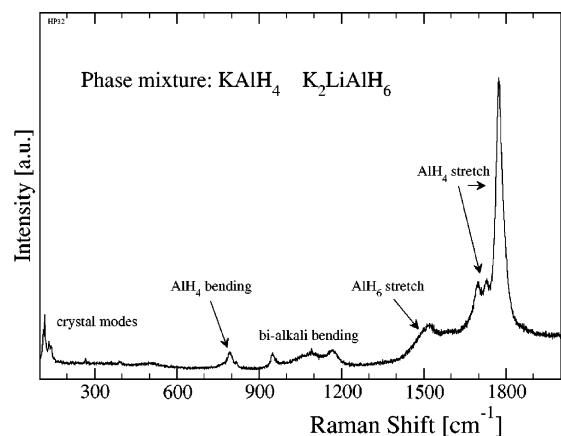


Figure 4. Raman spectrum of a sample containing a phase mixture of KAlH_4 and K_2LiAlH_6 . The AlH_6^{3-} stretching modes are clearly visible at 1500 cm^{-1} . The higher frequency Al–H stretching modes from the AlH_4^- anion are between 1675 and 1800 cm^{-1} and are similar to those found in NaAlH_4 .

Raman spectra were collected and compared to similar compounds in the literature. Figures 3 and 4 show Raman spectra from a sample of nearly phase pure K_2LiAlH_6 , and a KAlH_4 plus K_2LiAlH_6 mixture, respectively. On the basis of comparisons with calculations and experimental data taken for the NaAlH_4 compound,²⁸ the following tentative assignments are proposed. In the bialkali alanate sample (Figure 3), the Al–H stretch is located just above 1500 cm^{-1} , with the Al–H bending modes located roughly between 900 and 1200 cm^{-1} . The AlH_6^{3-} anion stretching vibrations in K_2LiAlH_6 are about 250–300 cm^{-1} below those of the AlH_4^- anion in KAlH_4 . This is a clear indication of a difference in coordination and bond strength of the Al–H bonds in the anions between the two compounds.

Figure 4 clearly shows three peaks in the Al–H stretching region in KAlH_4 . The modes appear to be the three predicted (E_g , A_g , and B_g) for the AlH_4^- anion stretch and are well separated and visible in KAlH_4 , in comparison to NaAlH_4 , where only two of the mode symmetries (A_g and E_g) are visible. This may be due to changes in the local environment of the anion, such as site symmetry and electron density, which will affect the vibrational mode intensities due to crystal field effects. The bialkali alanate anion bending and stretching modes are also visible in this spectrum as shown by comparison with Figure 3. The AlH_4 bending and crystal translation modes of KAlH_4 appear around 800 cm^{-1} , and below 200 cm^{-1} , respectively, in accordance with modes in NaAlH_4 .

TABLE 3: Wyckoff Positions from the VASP Relaxed HT- K_2LiAlF_6 -Type Structure

atom	Wyckoff position	x	y	z
Li	6c	0	0	0.4077
Al	3a	0	0	0
Al	3b	0	0	0.5
K	6c	0	0	0.1271
K	6c	0	0	0.2864
H	18h	0.4771	−0.4771	0.1273
H	18h	0.1509	−0.1509	0.0373

TABLE 4: Nearest-Neighbor Distances between Atoms in the HT- K_2LiAlF_6 -Type Structure after VASP Relaxation for Two Cases^a

pair	distances [Å]	
	(1) no interchange	(2) with interchange
Li–H	2.015	1.910
Al–H	1.765	1.750
K–H	2.820	2.530
Li–K	3.316	3.075
Li–Al	2.523	2.416
K–Al	3.422	3.213

^a (1) No interchange of Li and K Atoms. This case corresponds to the calculated lowest energy structure. (2) After interchanging the Li and K atoms and allowing the cell parameters and the ion positions to relax. All nearest-neighbor distances are in angstroms.

3.3. Ab Initio Calculations. Because of the large aspect ratio of the unit cell (c/a ratio of about 5), and the short Al–H distances from the Rietveld refinement, we performed ab initio total energy calculations, including relaxations, of the refined structure for comparison to database and other structures to further support the validity of the structure determination.

The Rietveld refined Al–H distances of 1.31–1.47 Å, as discussed in section 3.1, are short as compared to other alanates. This may be due to the low scattering factor of hydrogen in X-ray diffraction, leading to unreliable hydrogen atom positions, which are usually determined by collecting neutron diffraction spectra of a deuterated sample. Unfortunately, deuterated samples of K_2LiAlD_6 were not prepared due to the difficulty of preparing pure KD. We therefore performed ab initio relaxation of the hydrogen and metal atom positions. Wyckoff positions, and nearest-neighbor distances resulting from the relaxation of the Rietveld-refined structure using VASP, are shown in Tables 3 and 4, respectively. The Al–H-bonding distances are 1.77–1.79 Å, in agreement with the experimental values and ab initio relaxed values in the Na–Al–H system for the AlH_6^{3-} anion.²⁹ The VASP relaxed cell parameters are $a = 5.62$ and $c = 27.33$ Å, and agree with the experimentally determined values to within 0.01% and 0.3%, respectively.

The calculated total energies of structure types from the ICSD database are shown in Table 5. Two structures from the ICSD database share the same lowest energy. The first is $\text{Cs}_2\text{NaAlF}_6$, with a symmetry $C2/m$, and four formula units (f.u.) per cell. The second structure, K_2LiAlF_6 , is the high-temperature fluorite structure with symmetry $R\bar{3}m$, used as input in the Rietveld refinement, with six f.u./cell. The energies of the remaining structures from the ICSD database search are all at least 9.5 kJ/mol f.u. higher in energy. The energies, relative to the lowest two structures, K_2LiAlF_6 and $\text{Cs}_2\text{NaAlF}_6$, are listed in Table 5. The two models with lowest energy are assumed to be the most probable stable structures, ignoring contributions to the free energy due to phonons. Given structures of equal energy, the unit cell with the highest symmetry is usually chosen, and we check that this is indeed correct. To further compare the two

TABLE 5: Calculated Total Energies of K_2LiAlH_6 for Several Structure Types Taken from the ICSD Database^a

structure type	formula units per unit cell	ΔE [kJ/mol f.u.]	symmetry	space group no.
K_2LiAlF_6 ^{21,30}	6	0	$R\bar{3}m$	166
Cs_2NaAlF_6 ³¹	4	0	$C2/m$	12
K_3MoF_6 ³²	4	10.71	$Fm\bar{3}m$	225
Cs_2KTiF_6 ³³	4	10.81	$Fm\bar{3}m$	225
Na_2LiAlF_6 ³⁴	2	10.81	$P2_1/n$	14
Sr_2NiWO_6 ³⁵	2	10.81	$I4/m$	87
K_2LiAlF_6 ^{27,36}	4	10.90	$Fm\bar{3}m$	225
Si_2LiAlO_6 ³⁷	4	104.9	$C2/c$	14
Pb_2BiVO_6 ³⁸	4	104.9	$Pnma$	62

^a The formula units are given per conventional unit cell. The VASP energies are given relative to the lowest energy structure type, K_2LiAlF_6 . Symmetries and space group numbers are taken from the International Tables.

structures, X-ray diffraction patterns and pair distribution functions, shown in Figure 5, were calculated for each model. The pair distribution functions and calculated diffraction patterns are nearly identical. To quantify the difference, we calculate the Bragg residual between these two structures (as defined in the usual Rietveld method) with the calculated structure factors from the K_2LiAlH_6 phase playing the role of the observed intensities. Between 0 and $155^\circ 2\theta$, there are 155 and 163 structure factors for the K_2LiAlF_6 and Cs_2NaAlF_6 ICSD structures, respectively. Using a bin size of $0.15^\circ 2\theta$, there are 139 overlapping structure factors, yielding a Bragg R value of 7.2% between these two potential structures. A similar comparison with the other VASP relaxed structure types in Table 5 with K_2LiAlF_6 yields Bragg R values well over 50%, indicating that those structures will be much less likely candidates than Cs_2NaAlF_6 .

The Cs_2NaAlF_6 -type structure was then used as an input model for Rietveld refinements to compare this structure with the experimental data. By using the same instrumental parameters as in the refined model of the HT- K_2LiAlF_6 -type structure, and only changing the structural parameters, that is, space group, cell parameters, and atomic coordinates, the model was refined obtaining $R_B = 12.19\%$, which is significantly higher than the R_B -value obtained for the other structure model in section 3.1 ($R_B = 8.41\%$). A lower $R_B = 10.70\%$ was obtained by refining the coordinates for the K-atoms, but it was not possible to refine Li- or H-atoms. Thus, the Rietveld refinement validates the above conclusion that the HT- K_2LiAlF_6 -type structure best describes the structure of K_2LiAlH_6 .

To theoretically investigate possibilities to alloy this bialkali alanate, and thus tune its thermodynamic properties, the change in total energy due to cation mixing was calculated for one simple configuration change to estimate the energy penalty. Cation mixing in the bialkali alanate would tend to lower the free energy by increasing the entropy of the crystal. The standard expression for the ideal mixing (configurational) entropy for a binary alloy with $N_A + N_B = N$ is $S/N = -k_B[c \ln(c) + (1 - c) \ln(1 - c)]$, where $c = N_A/N$. If we consider the sub-lattice of cations only and assume that the Li and K ions are randomly mixed, we use $c = 1/3$, which amounts to $0.64 k_B$ per atom. At a temperature of 300 K, full mixing of the Li and K would lower the energy by about 4.3 kJ/mol f.u. However, the electronic energy would also be affected. We attempt to address the issue of cation mixing by performing a simple calculation where the positions of a Li and a K atom in the unit cell are exchanged. We allow the ion positions to move and also the cell volume and shape to relax. The atoms chosen for exchange were the Li ion at fractional coordinate (0,0,0.408) and the K

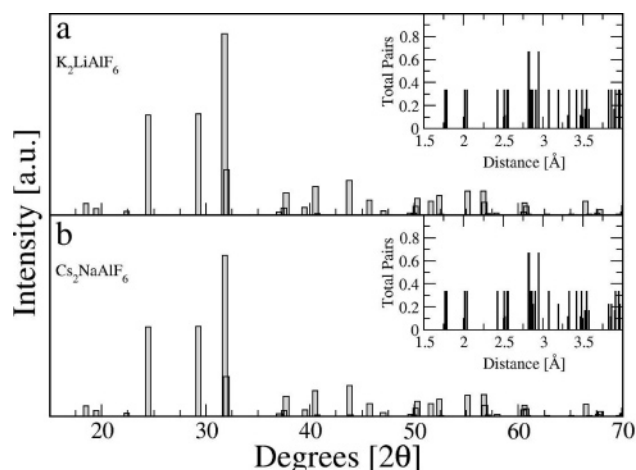


Figure 5. Calculated X-ray diffraction patterns for (a) the K_2LiAlF_6 structure, with space group $R\bar{3}m$, and (b) the Cs_2NaAlF_6 structure, with space group $C2/m$. The inset in each panel shows the calculated pair distribution function for the structures. A comparison of the two diffraction patterns yields a Bragg R value of about 7%.

ion at (0,0,0.127). The relaxation results in large atom movements and cell parameter changes, which lower the symmetry of the lattice from $R\bar{3}m$ to $P3m1$ (space group No. 156). The relaxed VASP total energy of the resulting structure is 28.9 kJ/mol f.u. higher in energy than that without the exchange. The cell volume increases dramatically from 748.35 to 784.66 Å³. The increase in electronic energy from swapping one pair of ions in the unit cell is almost 7 times larger than the lowering of the energy through the entropy of mixing. Table 4 contains the nearest-neighbor distances for the case of ion exchange. The largest changes in bonding distances are for K–Li and K–H. Assuming the effective charges on the Li and K ions, which we did not attempt to calculate, are roughly the same, suggests that the size difference between the K and Li atoms must impact the stability of the structure. This simple calculation indicates that cation mixing is highly unlikely in this bialkali alanate.

4. Conclusion

A new bialkali alanate, K_2LiAlH_6 , was synthesized and characterized. It was found to crystallize in space group $R\bar{3}m$ (No. 166) with unit cell parameters $a = 5.62068(8)$ and $c = 27.3986(6)$ Å being isostructural with the high-temperature form of K_2LiAlF_6 . Raman spectroscopy indicates that the Al–H stretching modes of the AlH_6^{3-} and AlH_4^- anions in K_2LiAlH_6 and $KAlH_4$, respectively, differ by about 250–300 cm⁻¹, and can be used to determine phase purity of samples. Ab initio total energy calculations were performed, including relaxations, of the Rietveld refined structure for comparison to database and other structures and to further support the validity of the structure determination. The calculations also indicate that the energy for the entropy of mixing of the cations is much smaller in magnitude than the increase in electronic energy, and therefore cation mixing is energetically unfavorable in this bialkali alanate. This suggests that tailoring the thermodynamics of complex type metal hydrides may not be possible in the same way as for the IMC hydrides.

Acknowledgment. Funding was provided by the U.S. Department of Energy, Office of Energy Efficiency and Renewable Energy under the Hydrogen Storage Grand Challenge, Center of Excellence within DOE's National Hydrogen Storage Project. We thank R. Baldonado for skillful technical assistance and V. Ozolins and R. Stumpf for useful discussions.

References and Notes

- (1) U.S. Department of Energy Hydrogen Program [http://www.hydrogen.energy.gov].
- (2) Sandrock, G. "State-of-the-art review of hydrogen storage in reversible metal hydrides for military fuel cell applications", Report prepared for the Office of Naval Research, under contract no. N00014-97-M-0001, 24 July, 1997.
- (3) Norskov, J. K.; Lyngby, J. K. *Europhys. News* **1988**, 19, 65.
- (4) Yvon, K. *Chimia* **1998**, 52, 613.
- (5) Morioka, H.; Kakizaki, K.; Chung, S.-C.; Yamada, A. *J. Alloys Compd.* **2003**, 353, 310.
- (6) Bogdanovic, B.; Schwickardi, M. *J. Alloys Compd.* **1997**, 253–254, 1.
- (7) Løvvik, O. M.; Swang, O. *Europhys. Lett.* **2004**, 67, 607.
- (8) Huot, J.; Boily, S.; Guthrie, V.; Schulz, R. *J. Alloys Compd.* **1999**, 383, 304.
- (9) Brinks, H. W.; Hauback, B. C.; Jensen, C. M.; Zidan, R. *J. Alloys Compd.* **2005**, 392, 27.
- (10) Graetz, J.; Lee, Y.; Reilly, J. J.; Park, S.; Vogt, T. *Phys. Rev. B* **2005**, 71, 184115.
- (11) Olofsson-Mårtensson, M.; Häussermann, U.; Tomkinson, J.; Noréus, D. *J. Am. Chem. Soc.* **2000**, 122, 6960.
- (12) Werner, P.-E.; Eriksson, L.; Westdahl, M. *J. Appl. Crystallogr.* **1985**, 18, 367.
- (13) Rodriguez-Carvajal, J. *Program FullProf.2k Version 3.20*; LLB JRC, February 2005.
- (14) Kresse, G.; Hafner, J. *Phys. Rev.* **1993**, B47, 558. Kresse, G.; Hafner, J. *J. Phys.: Condens. Matter* **1994**, 6, 8245. Kresse, G.; Furthmeuller, J. *Comput. Mater. Sci.* **1996**, 6, 15. Kresse, G.; Furthmeuller, J. *Phys. Rev. B* **1996**, 54, 111. Kresse, G. Ph.D. Thesis, Technische University Wien, 1993.
- (15) Perdew, J. P.; Burke, K.; Ernzerhof, M. *Phys. Rev. Lett.* **1996**, 77, 3865.
- (16) Inorganic Crystal Structure Database (ICSD) [http://icsd.ill.fr/icsd/].
- (17) Stokes, H. T.; Hatch, D. M. ISOTROPY, stokes.byu.edu/isotropy.html, 2002.
- (18) Werner, P.-E. *Ark. Kemi* **1969**, 31, 513.
- (19) *International Tables of Crystallography*, Vol. A, 2nd revised ed.; Kahn, T., Ed.; The International Union of Crystallography; D. Reidel Publishing Co.: 1987.
- (20) Sheldrock, G. M. *SHELXS97, Program for the Solution of Crystal Structures*; University of Göttingen: Germany, 1997.
- (21) Arndt, J.; Babel, D.; Haegeler, R.; Rombach, N. *Z. Anorg. Allg. Chem.* **1975**, 418, 193.
- (22) Brinks, H. W.; Hauback, B. C. *J. Alloys Compd.* **2003**, 354, 143.
- (23) Hauback, B. C.; Brinks, H. W.; Fjellvåg, H. *J. Alloys Compd.* **2002**, 346, 184.
- (24) Hauback, B. C.; Brinks, H. W.; Jensen, C. M.; Murphy, K.; Maeland, J. *J. Alloys Compd.* **2003**, 358, 142.
- (25) Rönnebro, E.; Noréus, D.; Kadir, K.; Reiser, A.; Bogdanović, B. *J. Alloys Compd.* **2000**, 299, 101.
- (26) Hauback, B. C.; Brinks, H. W.; Heyn, R. H.; Blom, R.; Fjellvåg, H. *J. Alloys Compd.* **2005**, 394, 35.
- (27) Graulich, J.; Drücke, S.; Babel, D. *Z. Anorg. Allg. Chem.* **1998**, 624, 1460.
- (28) Majzoub, E. H.; McCarty, K. F.; Ozoliņš, V. *Phys. Rev. B* **2005**, 71, 24118.
- (29) Ozolins, V.; Majzoub, E. H.; Udovic, T. J. *J. Alloys Compd.* **2004**, 375, 1.
- (30) Tressaud, A.; Darriet, J.; Lagassie, P.; Granec, J.; Hagenmuller, P. *Mater. Res. Bull.* **1984**, 19, 983.
- (31) Golovastikov, N. I.; Belov, N. V. *Kristallografiya* **1978**, 23, 42.
- (32) Toth, L. M.; Brunton, G. D.; Smith, G. P. *Inorg. Chem.* **1978**, 8, 2694.
- (33) Hoppe, R.; Becker, S. *Z. Anorg. Allg. Chem.* **1989**, 568, 126.
- (34) Ross, K. C.; Mitchell, R. H.; Chakhmouradian, A. R. *J. Solid State Chem.* **2003**, 172, 95.
- (35) Iwanaga, D.; Inaguma, Y.; Itoh, M. *Mater. Res. Bull.* **2000**, 35, 449.
- (36) Graulich, J.; Drueke, S.; Babel, D. *Z. Anorg. Allg. Chem.* **1998**, 624, 1460.
- (37) Redhammer, G. J.; Roth, G. *Kristallographie* **2004**, 219, 278.
- (38) Radosavljevic Evans, I.; Evans, J. S. O.; Howard, J. A. K. *J. Mater. Chem.* **2003**, 12, 2648.